

A synthetic example of anisotropic P -wave processing for a model from the Gulf of Mexico

Baoniu Han^{}, Tagir Galikeev[†], Vladimir Grechka^{*},*

Jérôme Le Rousseau^{} and Ilya Tsvankin^{*}*

^{}Center for Wave Phenomena, Department of Geophysics,*

Colorado School of Mines, Golden, CO 80401-1887

[†]Texaco North America Production, 4601 DTC Blvd.,

Denver, CO 80237

ABSTRACT

Transverse isotropy with a vertical symmetry axis (VTI media) is the most common anisotropic model for sedimentary basins. Here, we apply P -wave processing algorithms developed for VTI media to a 2-D synthetic data set generated by a finite difference code. The model, typical for the Gulf of Mexico, has a moderate structural complexity and includes a salt body and a dipping fault plane.

Using the Alkhalifah-Tsvankin dip-moveout (DMO) inversion method, we estimate the anisotropic coefficient η responsible for the dip dependence of P -wave NMO velocity in VTI media. In combination with the normal-moveout (NMO) velocity from a horizontal reflector [$V_{\text{nmo}}(0)$, the argument “0” refers to reflector dip], η is sufficient for performing all P -wave time-processing steps, including NMO and DMO corrections, prestack and poststack time migration. The NMO (stacking) velocities

needed to determine $V_{\text{nmo}}(0)$ and η are picked from conventional semblance velocity panels for reflections from subhorizontal interfaces, the dipping fault plane and the flank of the salt body. To mitigate the instability in the interval parameter estimation, the dependence of $V_{\text{nmo}}(0)$ and η on the vertical reflection time is approximated by Chebyshev polynomials with the coefficients found by “global” fitting of all velocity picks.

We perform prestack depth migration for the reconstructed anisotropic model and two isotropic models with different choices of the velocity field. The anisotropic migration result has a good overall quality, but reflectors are mispositioned in depth because the vertical velocity for this model cannot be obtained from surface P -wave data alone. The isotropic migrated section with the NMO velocity $V_{\text{nmo}}(0)$ substituted for the isotropic velocity also has the wrong depth scale and is somewhat inferior to the anisotropic result in the focusing of dipping events. Still, the image distortions are not significant because the parameter η , which controls NMO velocity for dipping reflectors, is rather small (the average value of η is about 0.05). In contrast, the isotropic section migrated with the vertical velocity V_0 has a poor quality (although the depth of the subhorizontal reflectors is correct) due to the fact that in VTI media V_0 can be used to stack neither dipping nor horizontal events. The difference between V_0 and the zero-dip stacking velocity $V_{\text{nmo}}(0)$ is determined by the anisotropic coefficient δ , which is greater than η in our model (on average, $\delta \approx 0.1$).

INTRODUCTION

Transverse isotropy with a vertical symmetry axis adequately describes elastic properties of shale formations and thin-bed sedimentary sequences (Thomsen, 1986; Sayers, 1994). Extending seismic processing to VTI media requires estimating anisotropic parameters from surface (preferably, P -wave) seismic data. Alkhalifah and Tsvankin (1995) showed that P -wave velocity analysis for models with a *laterally*

homogeneous VTI overburden above the target reflector can yield a single anisotropic parameter (η) in addition to the NMO velocity for horizontal events $V_{\text{nmo}}(\phi = p = 0)$ (ϕ is the reflector dip and p is the ray parameter of the zero-offset ray). In terms of Thomsen's (1986) parameters ϵ and δ and the P -wave vertical velocity V_0 , $V_{\text{nmo}}(0)$ and η are expressed as

$$V_{\text{nmo}}(0) = V_0 \sqrt{1 + 2\delta}, \quad (1)$$

and

$$\eta \equiv \frac{\epsilon - \delta}{1 + 2\delta}, \quad (2)$$

Obtained as functions of the vertical travelttime τ , $V_{\text{nmo}}(0)$ and η control all P -wave time-processing steps (NMO, DMO, time migration) needed to image reflectors beneath vertically inhomogeneous VTI media. Depth imaging (such as prestack depth migration), however, requires knowledge of the vertical velocity that cannot be determined from surface P -wave data alone. [Only if the VTI medium above the reflector is *laterally heterogeneous* (e.g., contains dipping interfaces), it may be possible to invert P -wave reflection moveout for the individual values of V_0 , ϵ and δ (Le Stunff et al., 1999; Grechka et al., 2000a,b).]

The interval values $V_{\text{nmo,int}}(p = 0, \tau)$ can be found using conventional Dix (1955) differentiation of NMO (stacking) velocities from horizontal (or subhorizontal) interfaces. To estimate the interval $\eta_{\text{int}}(\tau)$, Alkhalifah and Tsvankin (1995) and Alkhalifah (1997) developed a Dix-type differentiation algorithm operating with NMO velocities of dipping events. This procedure, however, is known to produce unreasonably strong variations in the interval η values (Alkhalifah and Rampton, 1997). We suggest to stabilize the inversion for interval η by representing the function $\eta_{\text{int}}(\tau)$ curve as a superposition of Chebyshev polynomials (Grechka et al., 1996). This allows us to take advantage of the redundancy in the available velocity picks and estimate only those (smooth) components of $\eta_{\text{int}}(\tau)$, which are necessary to fit the NMO velocity to a given degree of accuracy.

Alkhalifah-Tsvankin parameter-estimation methodology has been successfully used to perform anisotropic imaging in such exploration areas as offshore Africa (Alkhalifah et al., 1996) and Trinidad (Alkhalifah and Rampton, 1997), where massive shale formations are characterized by substantial (VTI) anisotropy. In both areas, accounting for vertical transverse isotropy leads to dramatic improvements in the imaging of dipping reflectors (fault planes) and helps to remove the distortions caused by nonhyperbolic moveout in the stacking of subhorizontal events. Similar benefits can be expected from VTI processing in the Gulf of Mexico (Meadows and Abriél, 1994; Bartel et al., 1998), where widespread mis-ties in time-to-depth conversion provide evidence of non-negligible anisotropy.

Here, we apply anisotropic processing to a 2-D synthetic data set generated by an anisotropic finite-difference code. The model used in our synthetic test was fashioned after a typical cross-section from the Gulf of Mexico (J. Leveille and F. Qin, pers. comm.) and contains a number of VTI layers. Although the structural complexity of the model is moderate, it includes a salt dome surrounded by sedimentary layers and a relatively steep fault plane (Figure 1). The anisotropic parameters can be considered as “best-guess” values that may well understate the magnitude of anisotropy in many areas of the Gulf of Mexico.

After the parameter-estimation step based on the modified Alkhalifah-Tsvankin method, we perform prestack depth migration of the data by means of a 45° finite-difference scheme (Han, 1998). First, the correct anisotropic model is used to generate a section that serves as a benchmark for comparison with other results. To simulate the output of a conventional processing sequence, we carry out isotropic migration with two different choices of the velocity function and discuss the distortions caused by the influence of anisotropy. Also, we interpolate and extrapolate the results of the anisotropic parameter estimation and perform depth migration with this approximate anisotropic model (assuming that the vertical velocity is equal to the zero-dip NMO

velocity). Although the model is weakly anisotropic, the VTI images have a superior quality, especially in the focusing and positioning of the fault plane.

PARAMETER ESTIMATION

Methodology

Suppose a dipping reflector is embedded in a vertically inhomogeneous VTI medium. The effective normal-moveout velocity and one-way zero-offset traveltimes for such a model are given by (Appendix A)

$$V_{\text{nmo,eff}}^2(p, \tau) = -\frac{1}{t(p, \tau)} \int_0^\tau V_0(\xi) q''(\xi) d\xi, \quad (3)$$

and

$$t(p, \tau) = \int_0^\tau V_0(\xi) [q(\xi) - p q'(\xi)] d\xi. \quad (4)$$

In equations (3) and (4), p is the horizontal component of the slowness vector (the ray parameter) of the zero-offset ray, the integration variable ξ has the meaning of the one-way vertical traveltime (τ is the one-way vertical traveltime from the surface to the zero-offset reflection point), and $t(p, \tau)$ is the one-way traveltime along the zero-offset ray. The vertical slowness component $q \equiv q(p)$ and its derivatives $q' \equiv dq/dp$ and $q'' \equiv d^2q/dp^2$ can be obtained in an explicit form using the Christoffel equation.

A key result of Alkhalifah and Tsvankin (1995) is that both $V_{\text{nmo,eff}}(p, \tau)$ and $t(p, \tau)$ depend on only two combinations of interval parameters of VTI media – the zero-dip NMO velocity $V_{\text{nmo,int}}(0, \tau)$ and the parameter $\eta_{\text{int}}(\tau)$. Therefore, the measurements of the effective NMO velocity $V_{\text{nmo,eff}}(p, \tau)$ for two different dips (or for two values of p) can be inverted for $V_{\text{nmo,int}}(0, \tau)$ and $\eta_{\text{int}}(\tau)$.

In most cases, we can use horizontal events to determine the velocity $V_{\text{nmo,eff}}(p = 0, \tau)$ as a function of the vertical traveltime τ . Then, the interval values $V_{\text{nmo,int}}(0, \tau)$

can be found from the conventional Dix (1955) equation,

$$V_{\text{nmo,eff}}^2(0, \tau) = \frac{1}{\tau} \int_0^\tau V_{\text{nmo,int}}^2(0, \xi) d\xi. \quad (5)$$

Obtaining $V_{\text{nmo,int}}(0, \tau)$ from equation (5) essentially amounts to differentiating the effective velocities $V_{\text{nmo,eff}}(0, \tau)$, which inevitably leads to amplification of errors in velocity picking. To mitigate this instability, equation (5) can be solved by the technique described in Grechka et al. (1996). This approach is based on approximating the velocity picks by Chebyshev polynomials and finding the interval velocity $V_{\text{nmo,int}}(0, \tau)$ in the Chebyshev domain. The desired smoothness of the solution and the degree to which errors in the effective velocities propagate into the interval values can be regulated by choosing the appropriate number of polynomials.

Once the function $V_{\text{nmo,int}}(0, \tau)$ has been estimated, the interval parameter η can be found from the NMO velocity and zero-offset traveltimes of dipping events [equations (3) and (4)]. The input data include the triplets of the horizontal slowness p (reflection slopes on zero-offset sections), the corresponding zero-offset traveltimes t , and the effective NMO velocity $V_{\text{nmo,eff}}$. These triplets can be picked from the zero-offset time sections generated for a range of stacking velocities or from semblance velocity panels at a number of adjacent common-midpoint (CMP) locations. The time-varying function $\eta_{\text{int}}(\tau)$ is represented as a sum of Chebyshev polynomials and reconstructed from the triplets $\{t, p, V_{\text{nmo,eff}}\}$ using equations (3) and (4) in the following way. For a trial solution $\eta_{\text{int}}(\tau)$ (specified at each iteration) and the zero-offset traveltimes $t(p, \tau)$ of a particular velocity pick, we find the corresponding vertical time τ using equation (4). Next we calculate the velocity $V_{\text{nmo,eff}}(p, \tau)$ from equation (3) and find the difference between the computed and measured values. Then $\eta_{\text{int}}(\tau)$ is updated to find the model that provides the best fit to all picked values $V_{\text{nmo,eff}}(p, \tau)$.

Data processing

The parameter-estimation algorithm described above was applied to a 2-D data set computed by finite differences for the VTI model shown in Figure 1. The section contains a salt body and a fault plane, which produce dipping events needed to estimate the parameter η . Judging by the magnitude of the coefficients ϵ and δ , some of the intervals may be considered as moderately or even strongly anisotropic, with the parameter ϵ approaching 0.3 in a thin layer at a depth of about 4.5 km (see Figure 1b). The average value of δ , however, is only about 0.1. Also, the key time-processing parameter η [equation (2)] is relatively small throughout the model, with a maximum value of 0.09 and average close to 0.05 (Figure 1d). Whereas such η values are not expected to cause serious problems in the focusing of reflection events, it is still instructive to evaluate possible image distortions and the performance of isotropic algorithms for such “quasi-elliptical” VTI media, which have moderate values of δ .

The function $\eta_{\text{int}}(\tau)$ was obtained as follows:

- Common-shot gathers were resorted into common-midpoint (CMP) gathers. Since the inversion algorithm needs moveout of dipping events to estimate η , we used only those CMP gathers which contain reflections from the top of the salt body (CMP locations from 4.9 to 6.7 km) and from the fault plane (CMP locations from 11.0 to 16.8 km). Thus, only about 30% of the data (Table 1) were actually included in the anisotropic parameter estimation.
- Conventional semblance analysis was used to obtain $V_{\text{nmo,eff}}(0, \tau)$ from subhorizontal events and the triplets $\{t, p, V_{\text{nmo,eff}}\}$ from the reflections from the right flank of the salt body and the fault plane. The ray parameter (horizontal slowness) p for dipping events was determined using the lateral time shift of the corresponding semblance velocity maxima.
- The parameter-estimation algorithm described above [based on equations (3)–(5)] was applied to invert the zero-dip velocities $V_{\text{nmo,eff}}(0, \tau)$ and the triplets $\{t, p, V_{\text{nmo,eff}}\}$

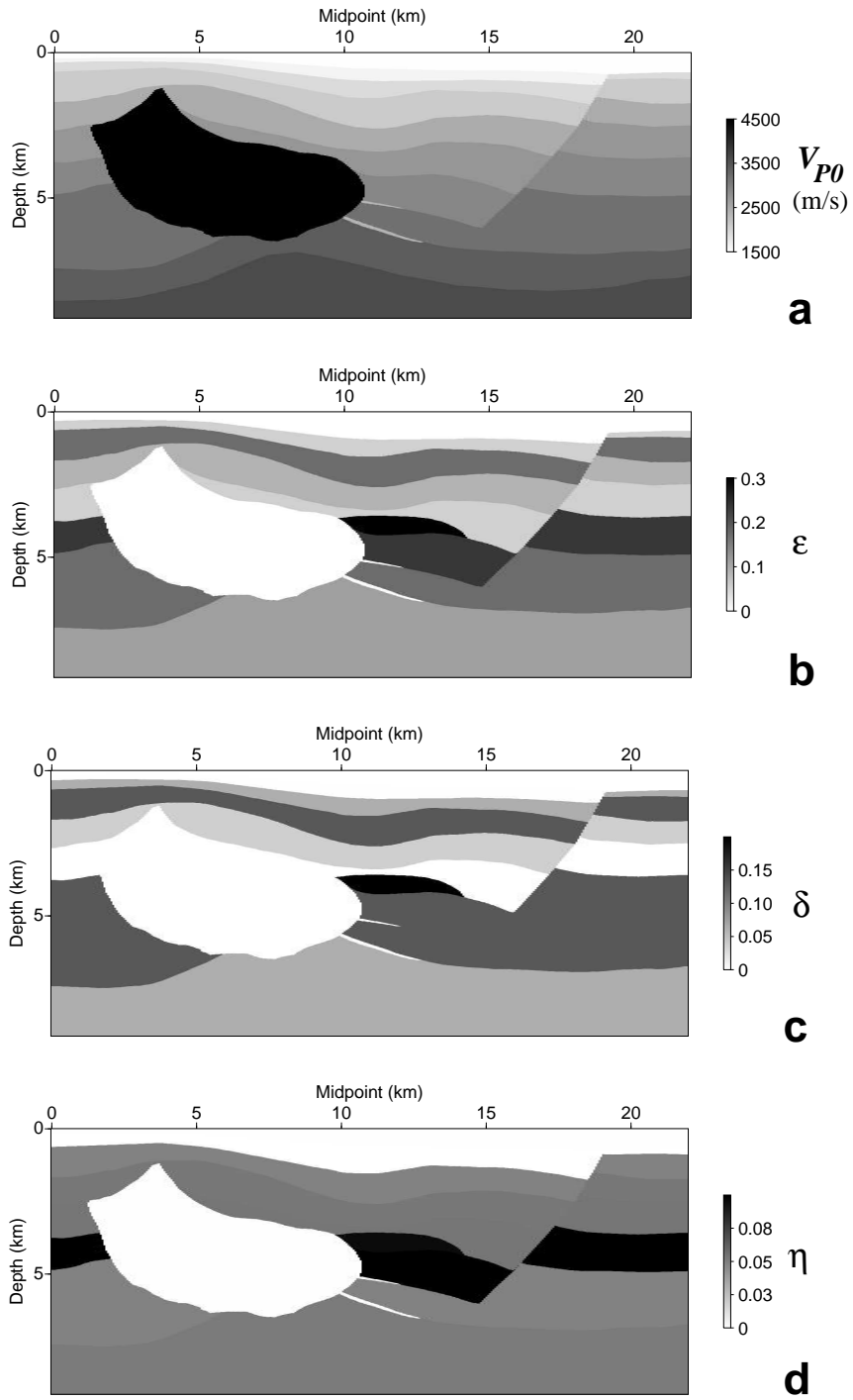


FIG. 1. Depth section showing parameters of the Amerada VTI model: (a) the P -wave vertical velocity V_0 ; (b) and (c) the Thomsen (1986) anisotropic parameters ϵ and δ ; (d) the Alkhalifah-Tsvankin parameter η .

for the interval values $V_{\text{nmo,int}}(0, \tau)$ and $\eta_{\text{int}}(\tau)$.

Model size:	21,945 m \times 9,144 m
Number of shots:	361
Shot spacing:	61 m
Number of receivers per shot:	500
Receiver spacing:	12.2 m
Dominant frequency:	20 Hz
Recording time:	8 s
Sample rate:	4 ms
Aperture for modeling:	-3,048 m to +6,096 m

Table 1. Parameters used in the finite-difference modeling.

There are two main sources of distortions in the estimation of the interval values of V_{nmo} and η : incorrect model assumptions and errors in velocity picking. The inversion procedure is designed for laterally homogeneous media above each dipping reflector, whereas in our model most “subhorizontal” interfaces have dips up to 15° . Ignoring the dips in evaluating $V_{\text{nmo}}(0)$ for this model leads to velocity errors (estimated from the isotropic cosine-of-dip dependence of NMO velocity) reaching 3.5%.

Uncertainty in the velocity picking for dipping events may give rise to errors of similar magnitude. Figure 2 displays a typical CMP gather located at 15.0 km and the corresponding semblance panel. The arrival reflected from the fault plane is recorded at a zero-offset time of 3.85 s. Apparently, this reflection has a much higher stacking (NMO) velocity than those of the subhorizontal events near zero-offset times of 3.67 s and 4.05 s (Figure 2b). Partly due to the interference with the event at 3.67 s, the fault-plane reflection produces a relatively broad semblance maximum (Figure 2a) covering approximately 0.15 km/s along the velocity axis. As a result, we can expect

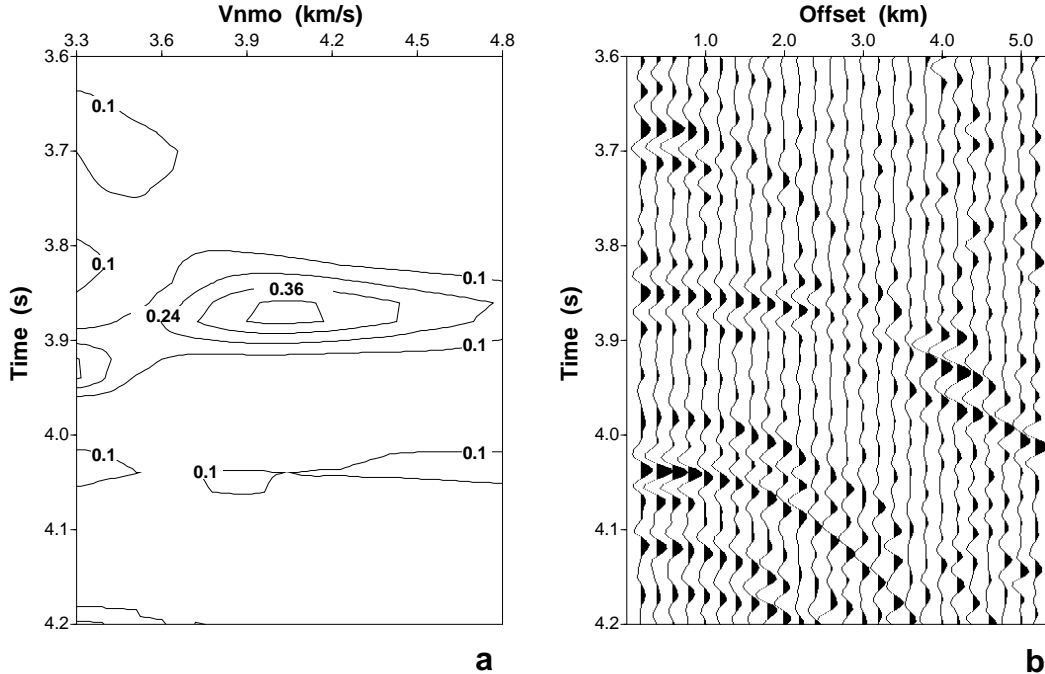


FIG. 2. Typical semblance panel (a) and the corresponding CMP gather (b).

the uncertainty in velocity picking of about 3–4%.

Naturally, this error propagates into the interval values of V_{nmo} and η with amplification, thus causing instability in the straightforward Dix-type differentiation. Application of Chebyshev polynomials, however, amounts to a smoothing operation that helps to stabilize the inversion procedure and eliminate spurious points on the interval curves.

Parameter-estimation results

The curves $V_{\text{nmo, int}}$ and η_{int} obtained as functions of the two-way vertical traveltimes for the left portion of the model are shown in Figure 3. The zero-dip NMO velocity was determined by semblance velocity analysis of subhorizontal events, while η was estimated using the NMO velocities and zero-offset traveltimes of reflections from the right flank of the salt body (Figure 1). Due to the regularization (smoothing) properties of our inversion algorithm, the curve $\eta_{\text{int}}(\tau)$ represents a sufficiently

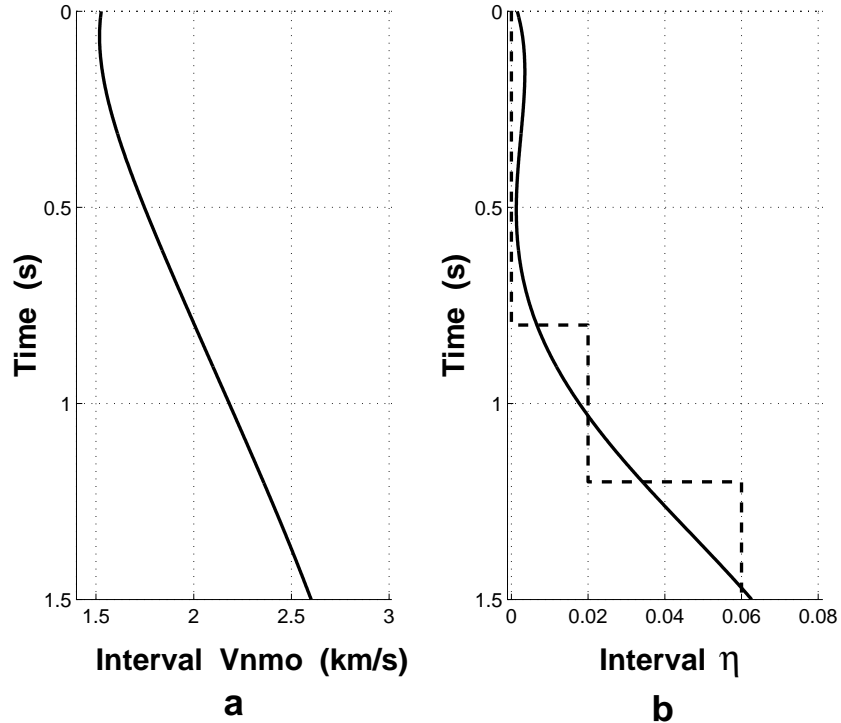


FIG. 3. Interval values of (a) V_{nmo} and (b) η (solid lines) estimated as functions of the two-way vertical traveltime using reflections from subhorizontal interfaces and from the right flank of the salt body. The velocity analysis was performed for CMP locations from 4.9 to 6.7 km. The dashed line shows the correct η -function for location 5.4 km.

accurate but smoothed version of the actual discontinuous η -function (dashed line in Figure 3b).

Figure 4 displays the inversion results for the right side of the model, obtained using reflections from the dipping fault plane. In this case, we were unable to detect the low- η layer at a vertical time of 3 s (Figure 4b), which was too thin to produce a noticeable change in the effective stacking (NMO) velocity (for the level of velocity errors described above). Apart from this problem, the algorithm adequately reconstructed the low-frequency trend of the interval function $\eta_{int}(\tau)$.

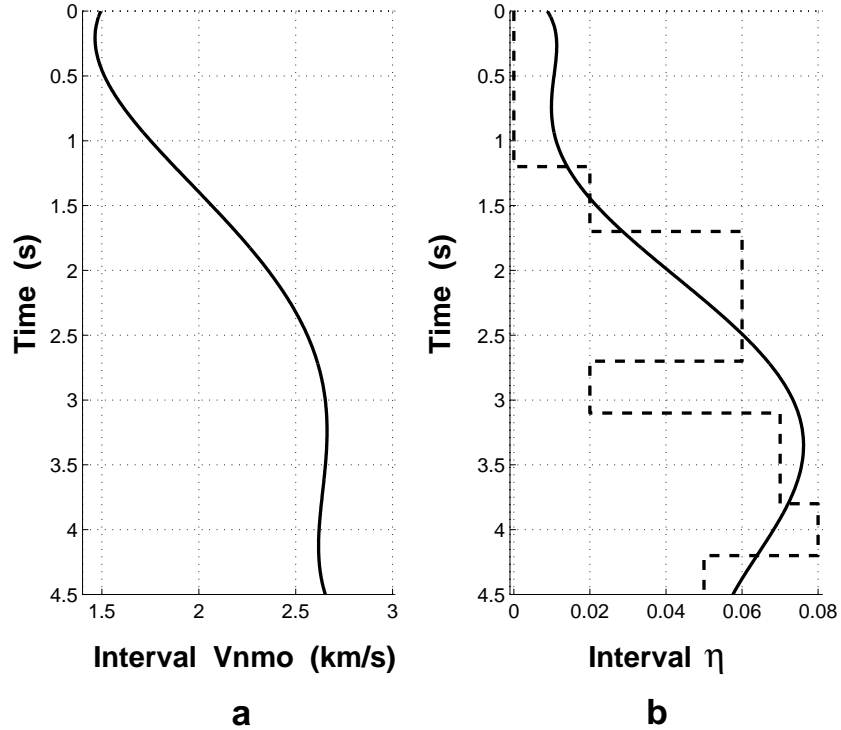


FIG. 4. Interval values of (a) V_{nmo} and (b) η (solid lines) estimated using reflections from subhorizontal interfaces and from the fault plane. The velocity analysis was performed for CMP locations from 11.0 through 16.8 km. The dashed line shows the correct η -function for location 13.8 km.

DEPTH MIGRATION

To resolve the vertical velocity needed for depth migration, P -wave reflection moveout for our model has to be combined with other data, such as reflection traveltimes of shear or converted waves; this joint inversion was not attempted on this data set. Nonetheless, we carried out prestack depth migration to evaluate image distortions caused by replacing the correct anisotropic velocity field with the following models:

1. Anisotropic model with the inverted η and the “best-guess” vertical velocity equal to the zero-dip NMO velocity.
2. Purely isotropic model with the velocity equal to either the zero-dip NMO velocity

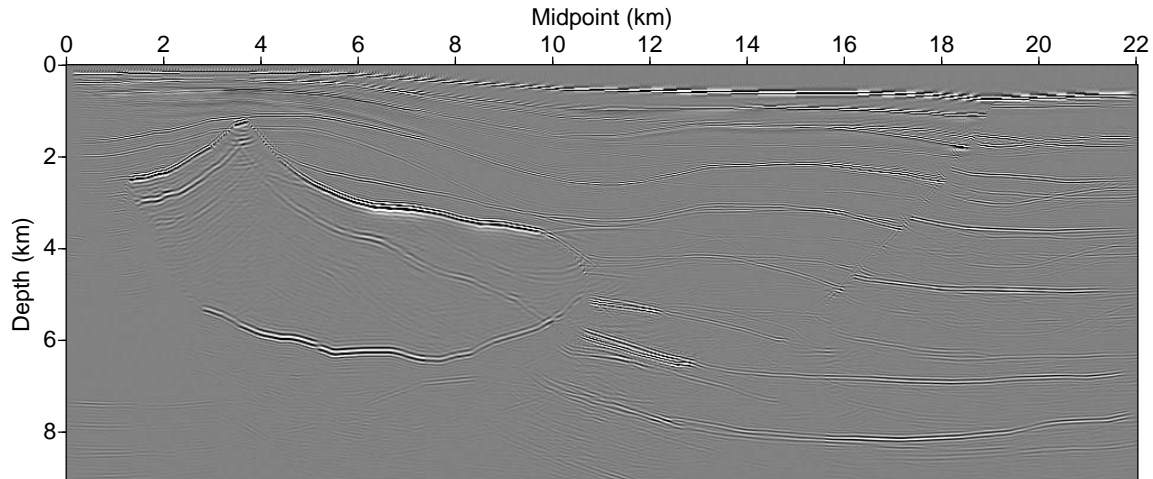


FIG. 5. Prestack depth migration for the correct anisotropic model.

or the actual vertical velocity.

We used an extension to VTI media of the migration algorithm of Han (1998) based on a 45° finite-difference scheme. Figure 5 shows a section obtained by prestack depth migration of the data using the correct VTI model from Figure 1. Both the salt body in the left part of the model and the fault plane are imaged reasonably well (also, see the close-up in Figure 6a). The left part of the bottom of the salt body, however, is almost invisible because of the limited recording aperture (Table 1). Also, some of the multiple arrivals, such as those inside the salt, were only partially attenuated in the stacking of the migrated data.

The migrated images in Figures 7 and 6b were obtained for an anisotropic velocity model based on the parameter-estimation results described above. Since the time-dependent η function was determined for only two ranges of CMP locations, the η section was built by interpolating and extrapolating the curves from Figures 3b and 4b. This smoothed and rather crudely interpolated version of the actual η field, however, did not cause a degradation in the quality of image, except for a slight deterioration in the focusing of the fault plane [compare sections (a) and (b) in Figure 6].

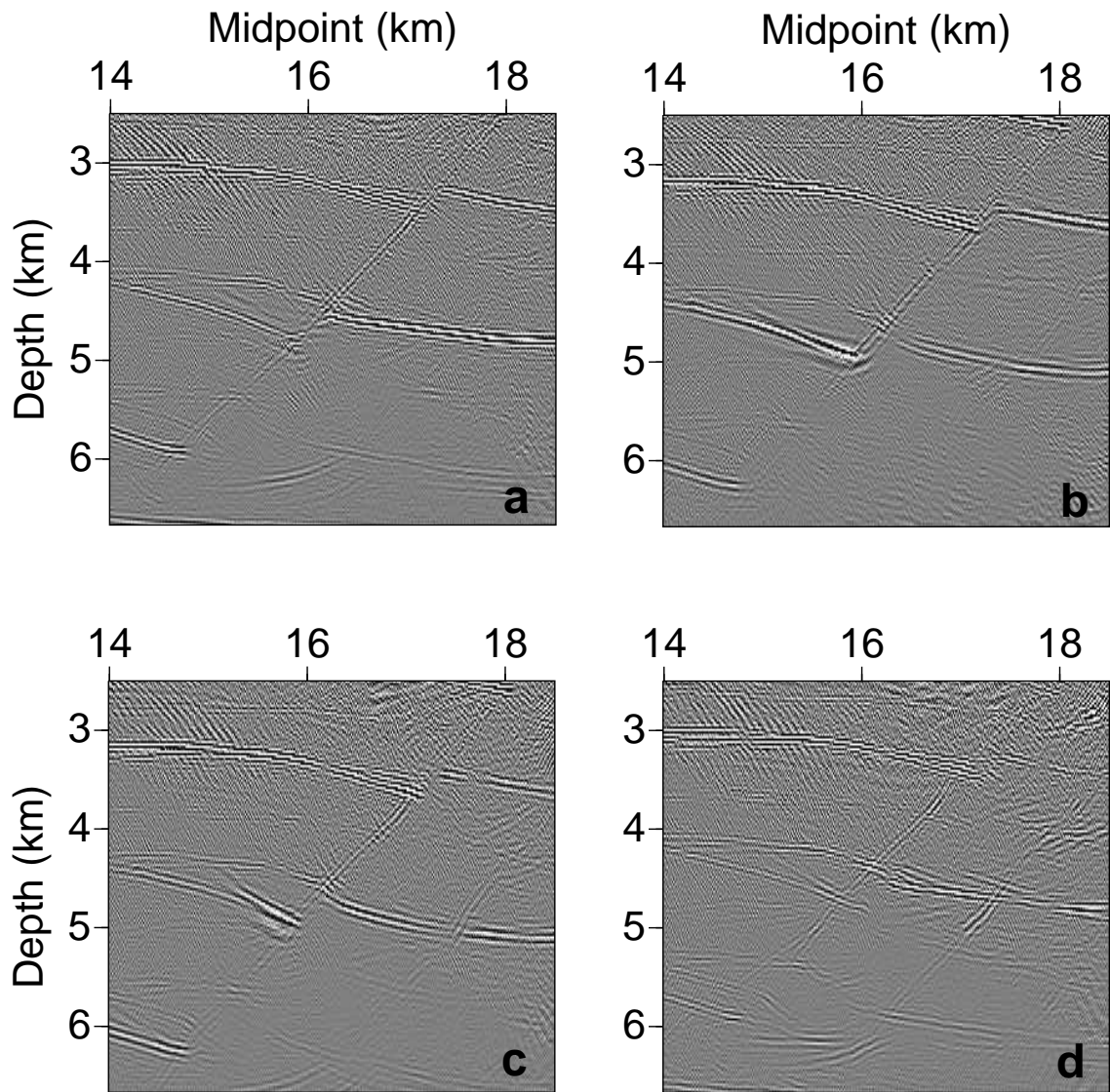


FIG. 6. Comparison of migration results for an area near the fault plane. (a) Anisotropic migration for the correct model; (b) anisotropic migration using the estimated parameters; (c) isotropic migration using the NMO velocity $V_{\text{nmo}}(0)$; (d) isotropic migration using the vertical velocity V_0 .

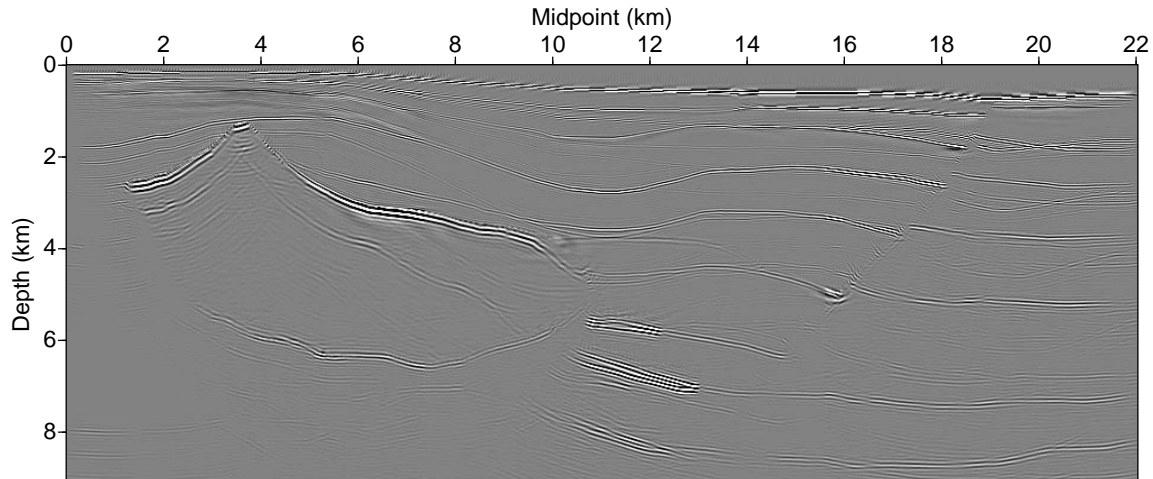


FIG. 7. Migration using an anisotropic model obtained by interpolation and extrapolation of the inverted functions η_{int} [Figures 3 and 4]. The vertical and NMO velocity are taken equal to each other ($\delta = 0$).

Clearly, fine details of the η -section do not have much influence on the migration results. Also, the magnitude of η in the model was so small (on average, $\eta \approx 0.05$, Figure 1d) that high accuracy in restoring η was unnecessary.

To specify the vertical velocity for the anisotropic migration in Figures 7 and 6b, we assumed that the parameter $\delta = 0$ [i.e., $V_0 = V_{\text{mmo}}(0)$], which leads to the incorrect depth scale for the whole image. It is clear from equation (1) that the percentage depth error in Figure 7 should be close to the average value of δ above the reflector. Indeed, the depth of subhorizontal reflectors in the lower right part of Figure 7 is overstated by about 7%, while the average δ in this part of model is about 0.1 (Figure 1c). Except for the depth error, the image in Figure 7 is quite close to the benchmark section from Figure 5. For more structurally complicated models, however, it may be necessary to know all three relevant parameters (V_0 , ϵ and δ) to ensure proper focusing of reflectors (Grechka et al., 2000a,b).

Figure 8 can be considered as the best possible output of the conventional isotropic processing sequence. The isotropic velocity model used to generate Figure 8 is based

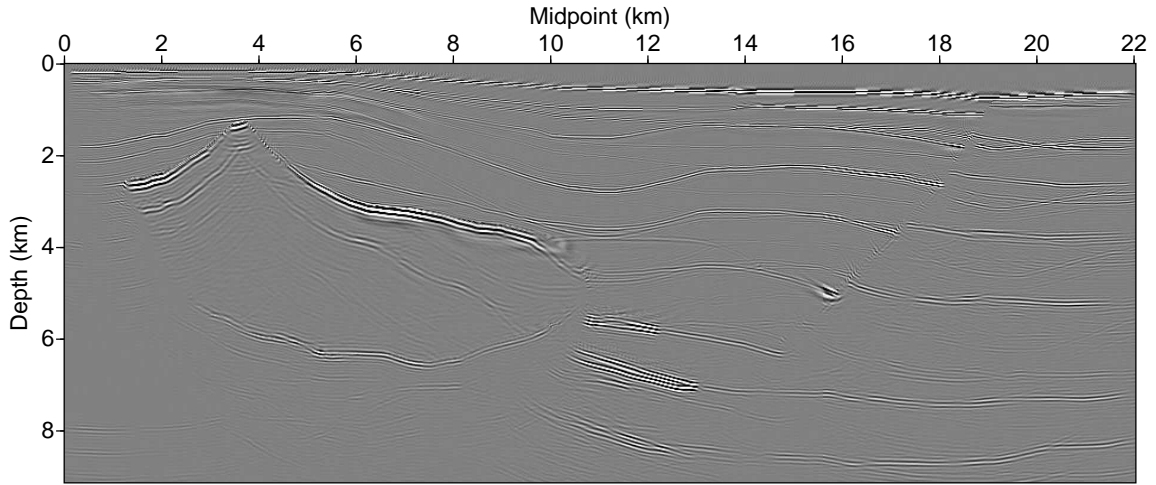


FIG. 8. Isotropic migration for a model with the medium velocity equal to the correct NMO velocity $V_{\text{nmo}}(0)$.

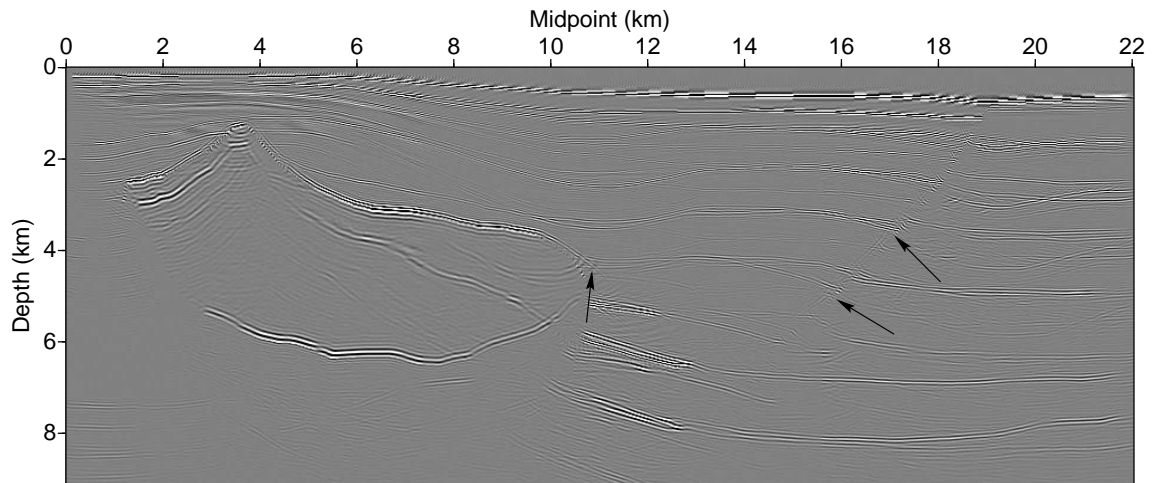


FIG. 9. Isotropic migration for a model with the velocity equal to the correct vertical velocity V_0 . The arrows mark some of the intersecting reflectors.

on the correct NMO velocity for horizontal reflectors conceivably obtained by error-free semblance velocity analysis. Comparing the lower right portions in Figures 8 and 5, we notice that the subhorizontal reflectors are mispositioned in depth, which was also the case in Figure 7. The overall quality of the image, however, is comparable to that in Figures 5 and 7. For example, there are no crossing features (conflicting dips) in the vicinity of the fault, which would have been indicative of the presence of anisotropy. The continuity and crispness of the fault-plane reflection are somewhat inferior to those in Figure 7, but the difference is not dramatic (compare Figures 6b and 6c). The acceptable quality of the isotropic result is explained by the small values of the η coefficient that controls the dip-dependence of NMO velocity in VTI media. Ignoring η in this model cannot cause substantial distortions in the stacking of dipping events, while the correct $V_{\text{nmo}}(0)$ ensures that the horizontal reflectors are focused well.

Another option in choosing the “isotropic” migration velocity is illustrated in Figures 9 and 6d. This time, the data were migrated using the correct vertical velocity V_0 , which in some cases may be obtained from check shots and well logs. As expected, all subhorizontal reflectors in Figures 9 and 6d are correctly positioned in depth. However, the quality of the image is considerably lower than that on the isotropic section migrated with the correct NMO velocity $V_{\text{nmo}}(0)$. The difference between V_0 and $V_{\text{nmo}}(0)$ causes misstacking of the subhorizontal events throughout the model. Since the wrong values of $V_{\text{nmo}}(0)$ also distort the NMO velocity of dipping events, the reflections from the fault plane (Figure 6d) and from the flank of the salt dome are poorly focused and positioned. Also notice the intersecting reflectors with different dips marked by arrows in Figure 9.

DISCUSSION AND CONCLUSIONS

This synthetic data test illustrates parameter-estimation and imaging issues for VTI media with a small time-processing parameter η (average $\eta \approx 0.05$) and a larger parameter δ (average $\delta \approx 0.1$) responsible for time-to-depth conversion. Combining NMO (stacking) velocities for subhorizontal and dipping events, we obtained the zero-dip NMO velocity $V_{\text{nmo}}(0)$ and the Alkhalifah-Tsvankin coefficient η (the two parameters needed for time imaging) as functions of the vertical reflection time. The inversion algorithm, based on the representation of both parameters through Chebyshev polynomials, allowed us to reduce the instability in the Dix-type differentiation and reconstruct the smooth components of the vertical variation in $V_{\text{nmo}}(0)$ and η .

Dipping reflections from a fault plane and the salt body were available over only two limited ranges of CMP locations on the left and right sides of the model (as is often the case in practice). Therefore, 1-D η -estimation could be carried out separately for those two groups of dipping events, with subsequent interpolation and extrapolation of the η -curves for the whole model. Although this procedure reconstructs only large-scale variations in η , a smoothed version of the η -field is usually sufficient for imaging purposes.

Depth migration of the inverted anisotropic velocity model produces a high-quality image close to that generated for the exact velocity field. Some inaccuracies in η estimation do not cause visible distortions in the focusing and positioning of reflection events, in part because the magnitude of η in the model is rather small. However, since the vertical velocity for this model cannot be determined from surface P -wave data, the image has the wrong depth scale (it was assumed that the vertical and NMO velocities were equal to each other).

The same mispositioning of subhorizontal events is observed on the depth section generated for a purely isotropic model with the velocity equal to the correct zero-

dip NMO velocity $V_{\text{nmo}}(0)$. Due to the small η -values, the overall image quality is comparable to that of the anisotropic section, except for some degradation in the focusing and continuity of the fault-plane reflection. Distortions in the isotropic image based on the correct zero-dip stacking velocity become significant only for models with average η values reaching or exceeding 0.1 (Alkhalifah et al., 1996; Alkhalifah, 1997).

Since the vertical velocity V_0 is needed to image horizontal events at the correct depth, the data were also migrated with the isotropic velocity model based on V_0 . Although reflector depths in this case are indeed accurate, both the horizontal and dipping reflections are poorly focused because in anisotropic media the vertical velocity is inappropriate for stacking reflection events of any dip. Note that the difference between the vertical velocity and the zero-dip NMO velocity is determined by the anisotropic coefficient δ , which is greater than η in this model.

Thus, application of isotropic depth migration in anisotropic media leads to inferior image quality and/or inaccurate positions of reflectors in depth. No single velocity is sufficient for generating a section with both good focusing and the correct spatial position of reflection events, even for layer-cake geometry. In models with moderate structural complexity, anisotropic migration with the correct inverted parameters $V_{\text{nmo}}(0)$ and η provides good focusing and positioning of reflection events, but may have the wrong depth scale. To obtain the vertical velocity and avoid depth errors in migration, P -wave reflection traveltimes in models with a laterally homogeneous VTI overburden should be supplemented by shear (or converted-wave) data or borehole information, such as check shots or well logs.

ACKNOWLEDGMENTS

We are grateful to Jacques Leveille of Amerada Hess for suggesting to perform this synthetic test and designing the model and Fuhao Qin (Amerada Hess) for generating the data using his finite-difference code. We also thank John Anderson (Mobil) and

John Toldi (Chevron) for their suggestion to use global smoothing of the triplets $\{t, p, V_{\text{nmo,eff}}\}$ to stabilize interval estimates of the parameter η . Editor Luc Ikelle and the reviewers made a number of useful suggestions which helped to improve the manuscript.

REFERENCES

- Alkhalifah, T., 1997, Seismic data processing in vertically inhomogeneous TI media: *Geophysics*, **62**, 662–675.
- Alkhalifah, T., and Rampton, D., 1997, Seismic anisotropy in Trinidad: Processing and interpretation: 67th Ann. Internat. Mtg., Soc. Expl. Geophys., Expanded Abstracts, 692–695.
- Alkhalifah, T., and Tsvankin, I., 1995, Velocity analysis in transversely isotropic media: *Geophysics*, **60**, 1550–1566.
- Alkhalifah, T., Tsvankin, I., Larner, K., and Toldi, J., 1996, Velocity analysis and imaging in transversely isotropic media: Methodology and a case study: *The Leading Edge*, **15**, no. 5, 371–378.
- Bartel, D.C., Abriel, W.L., Meadows, M.A, and Hill, N.R., 1998, Determination of transversely isotropic velocity parameters at the Pluto Discovery, Gulf of Mexico: 68th Ann. Internat. Mtg., Soc. Expl. Geophys., Expanded Abstracts, 1269–1272.
- Cohen, J.K., 1998, A convenient expression for the NMO velocity function in terms of ray parameter: *Geophysics*, **63**, 275–278.
- Dix C.H. 1955, Seismic velocities from surface measurements: *Geophysics*, **20**, 68–86.

- Grechka, V. and Tsvankin, I., 1999, 3-D moveout velocity analysis and parameter estimation for orthorhombic media: *Geophysics*, **64**, 820–837.
- Grechka, V., McMechan, G.A., and Volovodenco, V.A., 1996, Solving 1-D inverse problems by Chebyshev polynomial expansion: *Geophysics*, **61**, 1758–1768.
- Grechka, V., Pech, A., and Tsvankin, I., 2000a, Inversion of *P*-wave data in laterally heterogeneous VTI media. Part I: Plane dipping interfaces: 70th Ann. Internat. Mtg., Soc. Expl. Geophys., Expanded Abstracts, 2225–2228.
- Grechka, V., Pech, A., and Tsvankin, I., 2000b, Inversion of *P*-wave data in laterally heterogeneous VTI media. Part II: Irregular interfaces: 70th Ann. Internat. Mtg., Soc. Expl. Geophys., Expanded Abstracts, 2229–2232.
- Grechka, V., Tsvankin, I., and Cohen, J.K., 1999, Generalized Dix equation and analytic treatment of normal-moveout velocity for anisotropic media: *Geophysical Prospecting*, **47**, 117–148.
- Han, B., 1998, A comparison of four depth-migration methods: CWP Research Report (CWP-269).
- Le Stunff, Y., Grechka, V., and Tsvankin, I., 1999, Depth-domain velocity analysis in VTI media using surface *P*-wave data: Is it feasible?: 69th Ann. Internat. Mtg., Soc. Expl. Geophys., Expanded Abstracts, 1604–1607.
- Meadows, M., and Abriel, W., 1994, 3-D poststack phase-shift migration in transversely isotropic media, 64th Ann. Internat. Mtg., Soc. Expl. Geophys., Expanded Abstracts, 1205–1208.
- Sayers, C.M., 1994, The elastic anisotropy of shales: *J. Geophys. Res.*, **99**, No. B1, 767–774.
- Thomsen, L., 1986, Weak elastic anisotropy: *Geophysics*, **51**, 1954–1966.

Tsvankin, I., 1995, Normal moveout from dipping reflectors in anisotropic media: *Geophysics*, **60**, 268–284.

APPENDIX A: NMO VELOCITY AND ZERO-OFFSET TRAVELTIME IN VERTICALLY INHOMOGENEOUS VTI MEDIA

We consider reflection moveout in the dip plane of a reflector overlaid by a vertically inhomogeneous VTI medium. The goal of this appendix is to express both NMO velocity and zero-offset traveltimes through the interval values of the horizontal and vertical components of the slowness vector.

An exact expression for the dip-line NMO velocity in a symmetry plane of an anisotropic layer was given by Tsvankin (1995) and rewritten in terms of the components of the slowness vector by Cohen (1998):

$$V_{\text{nmo}}^2(p) = \frac{q''}{p q' - q}, \quad (\text{A-1})$$

where p and $q \equiv q(p)$ are the horizontal and the vertical components of the slowness vector, respectively, $q' \equiv dq/dp$, and $q'' \equiv d^2q/dp^2$; all quantities are evaluated for the zero-offset ray. The slowness vector can be obtained analytically by solving Christoffel equation, which reduces (for a given phase or slowness direction) to a cubic equation for the slowness-squared. The derivatives q' and q'' can be found in explicit form by differentiating the Christoffel equation. Equation (A-1) is a special case of a more general expression obtained by Grechka et al. (1999) for azimuthally varying NMO velocity in an arbitrary anisotropic layer above a dipping reflector.

The one-way traveltimes $t(p)$ along an oblique ray in a vertical symmetry plane of a homogeneous medium is given by (Grechka and Tsvankin, 1999)

$$t(p) = \tau V_0 (q - p q'), \quad (\text{A-2})$$

where τ is the one-way traveltimes along the vertical projection of the ray, and V_0 is the vertical velocity.

For vertically inhomogeneous media, the differential of the travelttime along a ray arc can be written as

$$dt(p) = V_0 (q - p q') d\tau . \quad (\text{A-3})$$

In the integral form, equation (A-3) yields

$$t(p, \tau) = \int_0^\tau V_0(\xi) [q(\xi) - p q'(\xi)] d\xi . \quad (\text{A-4})$$

According to Snell's law, the horizontal slowness p in equation (A-4) does not change along the ray.

To obtain NMO velocity in vertically inhomogeneous media, we apply the Dix-type averaging (Alkhalifah and Tsvankin, 1995) to equation (A-1):

$$V_{\text{nmo,eff}}^2(p, t(p, \tau)) = \frac{1}{t(p, \tau)} \int_0^t \frac{q''(\nu)}{p q'(\nu) - q(\nu)} d\nu , \quad (\text{A-5})$$

where integration is performed along the (generally oblique) zero-offset ray. To make equation (A-5) compatible with equation (A-4), it is convenient to use the vertical travelttime as the integration variable. Taking equation (A-3) into account, we represent equation (A-5) as

$$V_{\text{nmo,eff}}^2(p, \tau) = -\frac{1}{t(p, \tau)} \int_0^\tau V_0(\xi) q''(\xi) d\xi . \quad (\text{A-6})$$

Equations (A-4) and (A-6) express the NMO velocity and zero-offset travelttime in vertically inhomogeneous VTI media in a form convenient for moveout inversion.